

## Phonon anharmonicity of germanium in the temperature range 80–880 K

G. Nelin

*Royal Institute of Technology, Studsvik, Sweden*

G. Nilsson

*Aktiebolaget Atomenergi, Studsvik, Sweden*

(Received 20 November 1973; revised manuscript received 19 February 1974)

Phonon frequency shifts and linewidths in germanium have been studied in the temperature range 80–880 K by means of thermal neutron spectrometry. The results cannot be described in terms of the quasiharmonic approximation in which phonon frequencies are solely volume dependent. Theoretical calculations are found to be more satisfactory for the Raman frequency than for most other modes. A good account of the observed shifts is given by a proposal due to Barron, according to which the relative frequency renormalization of a crystal is proportional to the total harmonic vibrational energy. An analysis of the gradients of measured dispersion relations in the principal symmetry directions at 80 K is presented. It is shown that accidental degeneracies may influence the dispersion.

### I. INTRODUCTION

Experimental studies of anharmonic effects in crystalline germanium have been reported for specific heat, volume expansion, temperature and pressure dependence of the elastic constants, frequency shift, and line broadening of the Raman mode with increase of temperature. These effects are either average properties or long-wavelength-limit phenomena. By means of tunnel-junction techniques Payne<sup>1</sup> and Zavaritskii<sup>2</sup> observed phonon resonances as functions of pressure at 1 K at the reciprocal-lattice point  $L$  on the zone boundary. Measurements by the present authors of phonon frequencies all over the Brillouin zone and of linewidths for principal-symmetry-direction modes in germanium at 80 K have been published elsewhere.<sup>3,4</sup> (Some of these results are illustrated in Fig. 3.) Brockhouse and Dasannacharya<sup>5</sup> measured miscellaneous modes at 100 and 700 K and reported observations of frequency shifts.

Few theoretical studies of anharmonicity have been made on germanium and related solids. Dolling and Cowley<sup>6</sup> calculated Grüneisen parameters in germanium assuming only first-neighbor central anharmonic force constants which were determined by a fit to thermal-expansion data. Cowley<sup>7</sup> used the same model to generate frequency shifts and widths of the Raman line with a rise of temperature. The predicted shifts have subsequently proved to be in good agreement with experimental results. Jex<sup>8</sup> extended the model of Dolling and Cowley to include second-neighbor central interactions. Linewidths at 300 K were calculated for the branches  $\Delta'_2$ ,  $\Delta_5(A)$ , and  $\Lambda_3(A)$  together with some frequency shifts for the  $\Delta$  and the  $\Lambda$  branches. The results show a considerable frequency renormalization for transverse-acoustic modes around the zone boundary. The characteristic difference

between diamond and germanium as regards the dispersion of these branches should thus, to a great part, be due to anharmonic effects. Subsequently, Jex<sup>9</sup> has reported calculations of phonon linewidths at 80 K for all branches in the principal symmetry directions. These results are in fair agreement with experiment<sup>3</sup> except for the acoustic branch  $\Sigma_3(A)$ , in which case there is a considerable discrepancy.

In the present paper we present experimental results of frequency shifts and linewidths for phonon modes at  $\Gamma$ ,  $X$ , and  $L$  in germanium in the temperature range 80–880 K. The data are also analyzed and compared with other theoretical and experimental results.

### II. EXPERIMENTAL

The present experiment was carried out using a double-monochromator crystal spectrometer<sup>10</sup> and the 50-MW research reactor  $R2$  at Studsvik. In most respects the procedures adopted and the resolutions applied were identical with those described in Ref. 3. Optic modes were, however, not observed with a resolution as good as that previously obtained because the monochromator of the present instrument was restricted to Cu (220) reflections. [In the previous work (420 reflections were also available.) Typical figures for the energy resolution of optic modes were 0.30–0.40 THz for modes with vanishing frequency gradients. This had, however, an almost negligible influence on the accuracy of the recorded frequencies of the modes considered in the present work.

The intrinsic phonon linewidths of germanium are small and, in consequence, their extraction from the observed peak widths requires very good counting statistics. At temperatures above 300 K this requirement was not fulfilled except for trans-

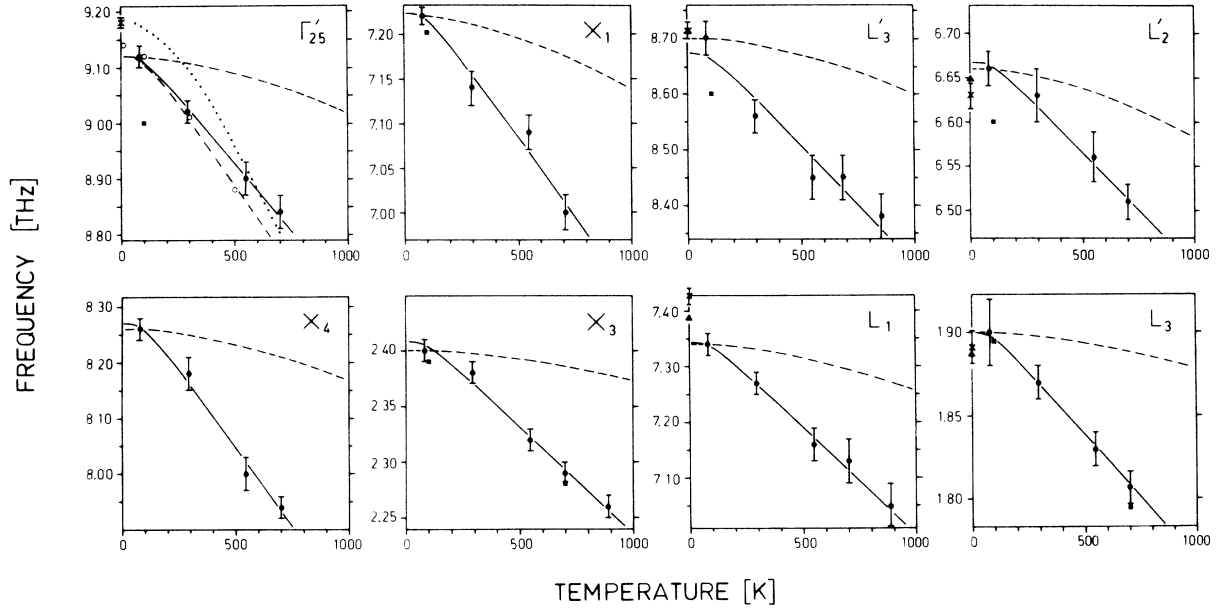


FIG. 1. Phonon frequencies vs temperature as obtained by the present authors (filled circles), Payne (Ref. 1) (filled triangles), Zavaritskii (Ref. 2) (crosses), and Brockhouse and Dasannacharya (Ref. 5) (filled squares). The errors quoted by Payne do not exceed the size of any of the filled triangles. Brockhouse and Dasannacharya listed no errors and their results are shown only when they lie within the frames of the figures. The dashed-dotted and the dotted curves represent the mean results of Raman scattering experiments by Cerdeira and Cardona (Ref. 11) and by Ray *et al.* (Ref. 12), respectively. The open circles mark the results of a calculation by Cowley (Ref. 7) when normalized to 9.01 THz at 300 K. The dashed curves represent the frequency variations as predicted by a quasiharmonic approximation (Ref. 14) when normalized to the present data at 80 K (see Sec. III B). The solid curves were obtained by least-squares fits of Eq. (5) to the present data.

verse-acoustic modes.

The germanium crystal was one-third the size of that used in Ref. 3 (from which it was cut). The crystal was mounted in a thermostat shielded so effectively as to limit temperature variations at the sample to a few degrees at 800 K.

### III. RESULTS AND DISCUSSIONS

#### A. Measured phonon frequencies

The modes studied were those of the symmetry points  $\Gamma$ ,  $X$ , and  $L$ . These are associated with most of the characteristic features of the phonon density-of-states spectrum<sup>4</sup> and they are accordingly significant for all phenomena dependent upon one- or two-phonon densities, such as, e.g., infrared absorption. The present results are plotted in Fig. 1. Brockhouse and Dasannacharya<sup>5</sup> found that the relative frequency shifts accompanying a change of temperature were approximately constant for all modes considered. This does not apply to the results obtained in the present work, where the relative shifts may vary by as much as one-third about their mean value. The actual values are  $-0.53(\Gamma'_{25})$ ,  $-0.54(L'_3)$ ,  $-0.52(L_1)$ ,  $-0.43(L'_2)$ ,  $-0.82(L_3)$ ,  $-0.75(X_4)$ ,  $-0.47(X_1)$ , and  $-0.86(X_3)$  when expressed as percent per 100 K.

By means of tunnel-junction techniques Payne<sup>1</sup> and Zavaritskii<sup>2</sup> observed phonon resonances in germanium at 1 K at the reciprocal-lattice point  $L$  and in the latter work even at  $\Gamma$ . The results are in fair agreement with those obtained at 80 K in the present experiment. The temperature dependence of the Raman-active mode  $\Gamma'_{25}$  has been studied by Cerdeira and Cardona<sup>11</sup> and by Ray *et al.*<sup>12</sup> The results of the present work are in best agreement with the former's data and also with those of a previous Raman scattering experiment by Parker *et al.*,<sup>13</sup> who reported the value 9.015 THz at 300 K (not shown in Fig. 1).

#### B. High-temperature frequencies

The frequency  $\nu_{\mathbf{q}j}$  of a vibrational mode is, in the general theory, a function of the mutually dependent thermodynamic variables  $P$ ,  $V$ , and  $T$ . We may write

$$\left(\frac{\partial \nu_{\mathbf{q}j}}{\partial T}\right)_P = \left(\frac{\partial \nu_{\mathbf{q}j}}{\partial T}\right)_V + \left(\frac{\partial \nu_{\mathbf{q}j}}{\partial V}\right)_T \left(\frac{\partial V}{\partial T}\right)_P. \quad (1)$$

In the harmonic approximation  $\nu_{\mathbf{q}j}$  is independent of  $T$ . The volume does vary with temperature, however, and in the so-called quasiharmonic approximation  $\nu_{\mathbf{q}j}$  is allowed to change with volume

TABLE I. High-temperature phonon-frequency derivatives in units of  $10^8 \text{ K}^{-1} \text{ sec}^{-1}$  for the modes studied in the present work. I, values obtained by least-squares fits of straight lines to the data in Fig. 1 above 80 K. II, same as for I from the quasiharmonic approximation as described in the text. III, values obtained by Zavaritskii (Ref. 2) and from high-temperature lattice expansivity and compressibility data. IV, the purely anharmonic contributions as obtained by means of Eq. (3) and columns I and III. V, same as for IV from Eq. (1) and columns I and II. The figures listed within parentheses in columns II, IV, and V are the absolute values of the ratios between the several derivatives and the frequencies, in units of  $10^{-4} \text{ K}^{-1}$ .

mode	$(\partial\nu_{\mathbf{q}j}/\partial T)_{P=0}$		$(-3\alpha/\chi)(\partial\nu_{\mathbf{q}j}/\partial P)_{T=1}$	$(\partial\nu_{\mathbf{q}j}/\partial T)_V$	
	I	II	III	IV	V
$\Gamma_{25}^h$	$-4.7 \pm 0.4$	$-1.3$ (0.15)	$-2.0 \pm 0.1$	$-2.7 \pm 0.5$ (0.30)	$-3.4 \pm 0.4$ (0.38)
$L_3^h$	$-4.6 \pm 0.6$	$-1.2$ (0.14)	$-2.0 \pm 0.1$	$-2.6 \pm 0.7$ (0.31)	$-3.4 \pm 0.6$ (0.40)
$L_1$	$-3.7 \pm 0.4$	$-1.0$ (0.14)	$-2.2 \pm 0.1$	$-1.5 \pm 0.5$ (0.21)	$-2.7 \pm 0.4$ (0.38)
$L_2^h$	$-2.8 \pm 0.4$	$-0.96$ (0.15)	$-0.5 \pm 0.1$	$-2.3 \pm 0.5$ (0.35)	$-1.8 \pm 0.4$ (0.26)
$L_3$	$-1.5 \pm 0.3$	$-0.27$ (0.15)	$+0.6 \pm 0.1$	$-2.1 \pm 0.4$ (1.15)	$-1.2 \pm 0.3$ (0.66)
$X_4$	$-6.0 \pm 0.5$	$-1.2$ (0.15)	...	...	$-4.8 \pm 0.5$ (0.60)
$X_1$	$-3.3 \pm 0.4$	$-1.0$ (0.14)	...	...	$-2.3 \pm 0.4$ (0.32)
$X_3$	$-2.0 \pm 0.3$	$-0.34$ (0.15)	...	...	$-1.7 \pm 0.3$ (0.73)

while the interaction between different modes is considered to be negligibly small. Thus  $(\partial\nu_{\mathbf{q}j}/\partial T)_V$  is a purely anharmonic term. The variation of  $\nu_{\mathbf{q}j}(V(T))$  has been calculated in the quasiharmonic approximation using the deformation dipole model developed by Tolpygo.<sup>14</sup> (The lattice-constant data were taken from Carr *et al.*<sup>15</sup> and from Gibbons<sup>16</sup> in the ranges 8–130 K and 130–300 K, respectively. Above 300 K the required values were obtained by extrapolation from the Gibbons data employing a fitted third-degree polynomial.) The results, normalized with respect to the present data at 80 K, are presented as dashed lines in Fig. 1. They show that the major part of the frequency shift is, according to Tolpygo's model, due to purely anharmonic effects. (A check of the accuracy of the calculated quasiharmonic frequencies is given in Sec. III D.)

By definition

$$\beta = 3\alpha = \left[ \frac{1}{V} \left( \frac{\partial V}{\partial T} \right)_P \right] \quad \text{and} \quad \chi = - \left[ \frac{1}{V} \left( \frac{\partial V}{\partial P} \right)_T \right], \quad (2)$$

where  $\alpha$  is the linear coefficient of thermal expansion and  $\chi$  the isothermal compressibility. Eqs. (1) and (2) give

$$\left( \frac{\partial\nu_{\mathbf{q}j}}{\partial T} \right)_P = \left( \frac{\partial\nu_{\mathbf{q}j}}{\partial T} \right)_V - \frac{3\alpha}{\chi} \left( \frac{\partial\nu_{\mathbf{q}j}}{\partial P} \right)_T, \quad (3)$$

where  $\alpha$  and  $\chi$  relate to the appropriate values of  $P$ ,  $V$ , and  $T$ . Inspection of Fig. 1 reveals that  $(\partial\nu_{\mathbf{q}j}/\partial T)_{P=0}$  is, within the limits of experimental error, a constant at higher temperatures. The quasiharmonic derivatives  $(\partial\nu_{\mathbf{q}j}/\partial T)_{P=0}^h$  seem not to be quite constant in this region but let us assume they are so. The anharmonic contribution  $(\partial\nu_{\mathbf{q}j}/\partial T)_V$  can then be obtained either from Eq. (1) via the identification  $(\partial\nu_{\mathbf{q}j}/\partial T)_P^h = (\partial\nu_{\mathbf{q}j}/\partial V)_T \times (\partial V/\partial T)_P$  or, if  $(\partial\nu_{\mathbf{q}j}/\partial P)_T$  is known, from Eq. (3). Zavaritskii<sup>2</sup> measured  $(\partial\nu_{\mathbf{q}j}/\partial P)_{T=1}$  for  $\Gamma_{25}^h$

and the modes at  $L$  under hydrostatic pressure. These derivatives, which were found to be independent of  $P$ , are applicable only if it is assumed they are constant in  $T$ . Table I demonstrates, however, that clear differences exist between  $(\partial\nu_{\mathbf{q}j}/\partial T)_{P=0}^h$  and  $(-3\alpha/\chi) \times (\partial\nu_{\mathbf{q}j}/\partial P)_{T=1}^{Zav}$ . (The compressibility data needed were taken from McSkimin.<sup>17</sup>) An experimental check would probably reveal that the assumption of temperature independence for  $(\partial\nu_{\mathbf{q}j}/\partial P)_T$  is invalid. It would be particularly interesting to check the postulated change of sign of this quantity for the mode  $L_3$  between the low- and the high-temperature regions.

Finally, columns II and V in Table I show that the frequency shifts with temperature due to volume expansion are constant, provided they are expressed in the form  $(\partial\nu_{\mathbf{q}j}/\partial T)_P/\nu_{\mathbf{q}j}$ , while the  $(\partial\nu_{\mathbf{q}j}/\partial T)_V/\nu_{\mathbf{q}j}$  for the purely anharmonic effects vary by a factor of 3 between the smallest and the largest value.

#### C. Barron's theory of frequency renormalization

Barron<sup>18</sup> proposed that the frequency renormalizations might be evaluated by assuming the relative shifts to be proportional to the harmonic vibrational energy of the crystal, i. e.,  $\partial\nu/\nu = A \langle E_{\text{vib}}^h \rangle$ . This may be written

$$\nu_{\mathbf{q}j}(T) = \nu_{\mathbf{q}j}^h \left[ 1 + \frac{1}{3Nk\Theta_{\mathbf{q}j}} \left\langle \sum_{\mathbf{q}j} h\nu_{\mathbf{q}j}^h (n_{\mathbf{q}j} + \frac{1}{2}) \right\rangle \right], \quad (4)$$

where  $\nu_{\mathbf{q}j}^h$  is the harmonic frequency and  $n_{\mathbf{q}j}$  is its Bose-Einstein distribution function. Barron's constant  $A$ , usually assumed to be identical for all modes, has been redefined to include a temperature,  $\Theta_{\mathbf{q}j}$ , characteristic of each mode. Feldman *et al.*<sup>19</sup> showed that for the nearest-neighbor central-force model Barron's proposal leads to an exact expression for the frequency shifts due to

the quartic term in the expansion of the lattice potential energy. The contributions from the cubic term were found to be exactly described in the high- and low-temperature limits. It is known that in a solid such as germanium bond-stretching forces between nearest neighbors dominate the interactions. Equation (4) should thus be expected to yield a good first approximation for most of the frequency renormalizations. Barron<sup>18</sup> also pointed out that a shift obtained from neutron scattering is the same as that obtained from the entropy but not to that obtained from the free energy. Although this relationship is not exact, as was shown by Horton,<sup>20</sup> the discrepancy is probably negligible for weakly anharmonic crystals like germanium. Thus the average vibrational energy in Eq. (4) may in the present case be replaced by  $3N\hbar\nu_g(n_g + \frac{1}{2})$ , where  $\nu_g$  is the geometric mean frequency associated with the entropy.  $\nu_g$  has been determined to  $5.110 \pm 0.015$  THz from specific-heat data by Flubacher *et al.*<sup>21</sup> and the value 5.11 THz was obtained from neutron scattering data.<sup>4</sup> Equation (4) then reads

$$\nu_{\mathfrak{q}j}(T) = \nu_{\mathfrak{q}j}^h \left[ 1 + \frac{\hbar\nu_g}{k\Theta_{\mathfrak{q}j}} \left( \frac{1}{e^{\hbar\nu_g/kT} - 1} + \frac{1}{2} \right) \right], \quad (5)$$

giving an absolute zero frequency

$$\nu_{\mathfrak{q}j}(0) = \nu_{\mathfrak{q}j}^h \left[ 1 + \frac{\hbar\nu_g}{2k\Theta_{\mathfrak{q}j}} \right]. \quad (6)$$

A fit of Eq. (5) to the present data by the method of least squares with  $\nu_{\mathfrak{q}j}^h$  and  $\Theta_{\mathfrak{q}j}$  as free parameters, presented in Fig. 1 and Table II, is found to be good. The data at 80 K are close to the harmonic spectrum. The  $\nu_{\mathfrak{q}j}(0)$ 's lie within the limits of experimental error, while the  $\nu_{\mathfrak{q}j}^h$ 's exceed the error limits by 0.03 THz, or 0.6% of  $\nu_g$ , on the average. The contributions to the frequency shifts from the cubic and the quartic terms in the expansion of the lattice potential are of opposite sign.<sup>22</sup> The negative values obtained for the  $\Theta_{\mathfrak{q}j}$ 's show that the cubic terms dominate. It is also noteworthy that these values are of the same magnitude as those characteristic of the temperatures corresponding to the energy differences between the lowest conduction-band and the highest valence-band levels.<sup>23</sup>

Cowley<sup>7</sup> calculated the renormalization of  $\Gamma'_{25}$  assuming nearest-neighbor central interactions and contributions only from third-order terms in the lattice potential. His results, normalized to 9.01 THz at 300 K, are represented in Fig. 1 by open circles. The temperature dependence is somewhat stronger than that found in the present work but still within the limits of error. The renormalization at absolute zero, roughly  $-0.05$  THz, is close to the present value of  $-0.06 \pm 0.02$

TABLE II. Harmonic ( $\nu_{\mathfrak{q}j}^h$ ) and anharmonic ( $\nu_{\mathfrak{q}j}(0)$ ) phonon frequencies in units of THz, and temperatures characteristic of the anharmonicity ( $\Theta_{\mathfrak{q}j}$ ) in degrees K as obtained from Eqs. (5) and (6).

mode	$\Gamma'_{25}$	$L'_3$	$L_1$	$L'_2$	$L_3$	$X_4$	$X_1$	$X_3$
$\nu_{\mathfrak{q}j}^h$	$9.181 \pm 0.009$	$8.726 \pm 0.035$	$7.391 \pm 0.008$	$6.700 \pm 0.009$	$1.919 \pm 0.003$	$8.340 \pm 0.017$	$7.267 \pm 0.013$	$2.431 \pm 0.007$
$\nu_{\mathfrak{q}j}(0)$	$9.120 \pm 0.009$	$8.673 \pm 0.035$	$7.343 \pm 0.008$	$6.668 \pm 0.009$	$1.899 \pm 0.003$	$8.270 \pm 0.017$	$7.223 \pm 0.013$	$2.407 \pm 0.007$
$\Theta_{\mathfrak{q}j}$	$-18500 \pm 900$	$-20300 \pm 3200$	$-18900 \pm 800$	$-25400 \pm 1800$	$-12300 \pm 500$	$-14500 \pm 900$	$-20200 \pm 2000$	$-12400 \pm 700$

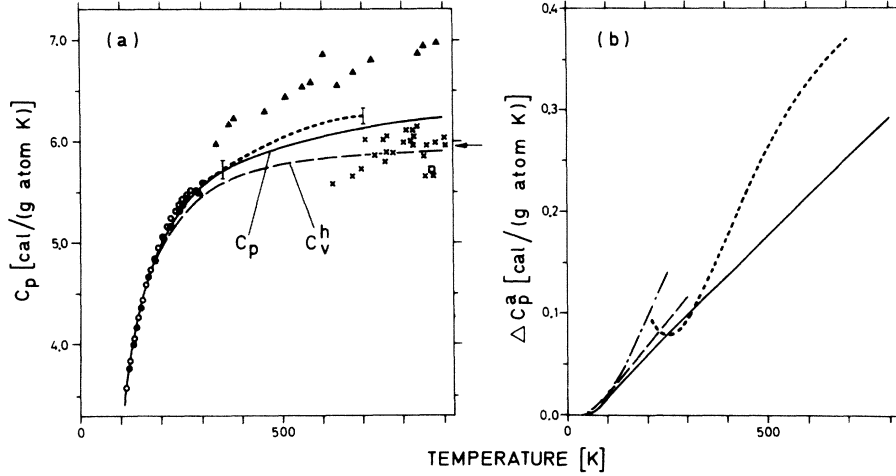


FIG. 2. (a) Specific heat at constant pressure,  $C_p$ , of germanium as obtained by Flubacher *et al.* (Ref. 21) (filled circles), Piesbergen (Ref. 26) (open circles), Smith (Ref. 28) (crosses), Greiner (Ref. 27) (open square), and Gerlich *et al.* (Ref. 29) (filled triangles). The dotted curve represents the mean of the results obtained by Chen and Turnbull (Ref. 25) and the bars indicate the maximum scattering of points. The curves labeled  $C_p$  and  $C_v^h$  show the results of calculations from the present data as described in Sec. III D. The arrow marks the value of the constant of Dulong and Petit. (b) The differences between three of the data sets in (a) and  $C_v^h$ , namely, for Flubacher *et al.* (dashed curve), Piesbergen (dashed-dotted curve), and Chen and Turnbull (dotted curve). The solid curve represents  $C_p - C_v^h$  of the present calculation.

THz. Jex<sup>8</sup> extended Cowley's model to include central forces with second nearest neighbors. His frequency-dependent renormalizations for the transverse-acoustic branches  $\Delta_5(A)$  and  $\Lambda_3(A)$  amount to roughly 10% at the zone boundary. The renormalizations of the remaining  $\Delta$  and  $\Lambda$  branches gave values which are one order of magnitude lower. The latter result is in fair agreement with the present findings while the former is in sharp contrast.

#### D. Specific heat

The specific heat at constant and vanishing pressure is given by the relationship<sup>24</sup>

$$C_p = T \left( \frac{\partial S}{\partial T} \right)_p. \quad (7)$$

If the phonon system is assumed to be weakly interacting it may be approximated to an ideal Bose gas. This yields the entropy<sup>24</sup>

$$S = k \sum_x \{ x / (e^x - 1) - \ln(1 - e^{-x}) \}, \quad x = h\nu_{\mathbf{q}j}(T) / kT. \quad (8)$$

Equations (5) and (6) may be written

$$\nu_{\mathbf{q}j}(T) = \nu_{\mathbf{q}j}(0) F(T), \quad F(T) = [1 + \gamma / (e^{h\nu_{\mathbf{q}j}/kT} - 1)]. \quad (9)$$

In Eq. (9) it is assumed that all modes are subject to the same percentage frequency shift with temperature. The actual value  $\gamma = -1.385 \times 10^{-2}$  is obtained from the mean value of  $\Theta_{\mathbf{q}j}$  in Table II. Standard procedures then yield

$$C_p = 3Nk \int_0^{\nu_{\max}} (y^2 \sinh^{-2} y) g(y) dy \left\{ 1 - \frac{F'(T)}{F(T)} T \right\},$$

$$y = h\nu F(T) / 2kTF(80). \quad (10)$$

The frequencies and the density of states are those obtained at 80 K.<sup>3,4</sup> The "harmonic" specific heat  $C_v^h$  (including the zero-point motions) is obtained from  $C_p$  by setting  $F(T) = F(80)$  and omitting the expression within the braces.

Figure 2(a) shows the results of the present calculation of  $C_p$  and  $C_v^h$  together with experimental data. The agreement of  $C_p$  with the well-established data of Piesbergen<sup>26</sup> and Flubacher *et al.*<sup>21</sup> and of  $C_v^h$  with the constant of Dulong and Petit, as well, is good. The results of Greiner,<sup>27</sup> Smith,<sup>28</sup> and Gerlich *et al.*<sup>29</sup> receive little support from the low-temperature data. The differences between the "best" specific-heat data and  $C_v^h$  is plotted in Fig. 2(b) together with the present values for  $C_p - C_v^h$ . If the results of Piesbergen were correct an error of about 80% is inferred for the present value of  $\Delta C_p^a$  at 270 K. The anharmonic contributions extracted from the data by Chen and Turnbull<sup>25</sup> exhibit smaller percentage deviations from the present results than those of Piesbergen but they have a strange shape, as can be seen even from Fig. 2(a). The deviations from the data of Flubacher *et al.* are considerably smaller and, moreover, these authors performed a calculation of  $C_v^h$  up to 300 K which gave results in excellent agreement with the present values of  $C_v^h$ . A definite statement of how well the mean frequency shift of the symmetry-point phonon modes represents the mean of all modes must, however, await more accurate high-temperature specific heat data.

Owing to volume expansion the specific heat re-

ceives a contribution<sup>24</sup>

$$C_P - C_V = \alpha^2 T v / \chi, \quad (11)$$

where  $v$  is the molar volume. At 300 K,  $C_P - C_V = 2.3 \times 10^{-2}$  (cal/g atom K), while the corresponding value obtained from the quasiharmonic shifts of the present study (see Sec. III B) is  $1.6 \times 10^{-2}$  (cal/g atom K). The difference is 7% of the total anharmonic contribution,  $\Delta C_P^a$ , and the errors of the calculated quasiharmonic shifts should therefore have no influence on the conclusions drawn in Sec. III B.

#### E. Phonon linewidths

A very striking feature of the present results is the lack of an evident broadening of the peak widths with temperature for the transverse-acoustic modes  $X_3$  and  $L_3$ . The widths observed only slightly exceed the calculated resolution widths. More noteworthy, however, is the fact that even the observed widths are smaller than theoretically estimated linewidth values. [It should be remembered that an observed peak is a convolution of the resolution function with the neutron cross section (phonon line).] At 300 K, for instance, Jex<sup>8</sup> predicts a linewidth of 0.23 THz for  $L_3$ , while the width of the observed peak is  $0.13 \pm 0.01$  THz. In the high-temperature limit, the linewidths are expected to vary approximately linearly with temperature. Then, if scaled to 700 K, the values of Jex would read 0.30 THz for  $X_3$  and 0.54 THz for  $L_3$ , while we have recorded  $0.13 \pm 0.01$  and  $0.12 \pm 0.01$  THz, respectively. We believe the phonon linewidths of these modes do not exceed a few units of

0.01 THz anywhere in the temperature region covered.

The rest of the modes considered were not very suitable for linewidth studies as a function of temperature because of insufficient counting statistics and, at the highest temperatures, multiphonon contributions and incoherent processes that interfered with the one-phonon resonances.

The valence-force-field model seems to be the best existing harmonic approximation to the lattice dynamics of germanium.<sup>30,31</sup> This model is founded on bond-stretching and angle-bending forces and interactions between them. The former are central two-body forces which operate between nearest neighbors and the latter are three-body forces which act between first and second nearest neighbors. In this theory the dynamics of transverse-acoustic branches are dominated by the angle-bending forces and the zone-boundary modes  $L_3$  and  $X_3$  are entirely governed by them. Angular forces were not included in the calculations by Jex. It is possible that omission of angular forces may lead to erroneous results for transverse-acoustic branches.

#### IV. ACCIDENTAL DEGENERACIES AND GRADIENTS

Kagan and Zhernov<sup>32</sup> used the Green's-function method to analyze the influence of anharmonicity on phonon dispersion near a point of accidental degeneracy. It was found that modes involved in such a degeneracy may have different renormalizations and lifetimes. Even when branches come close to one another, without actually intersecting, they

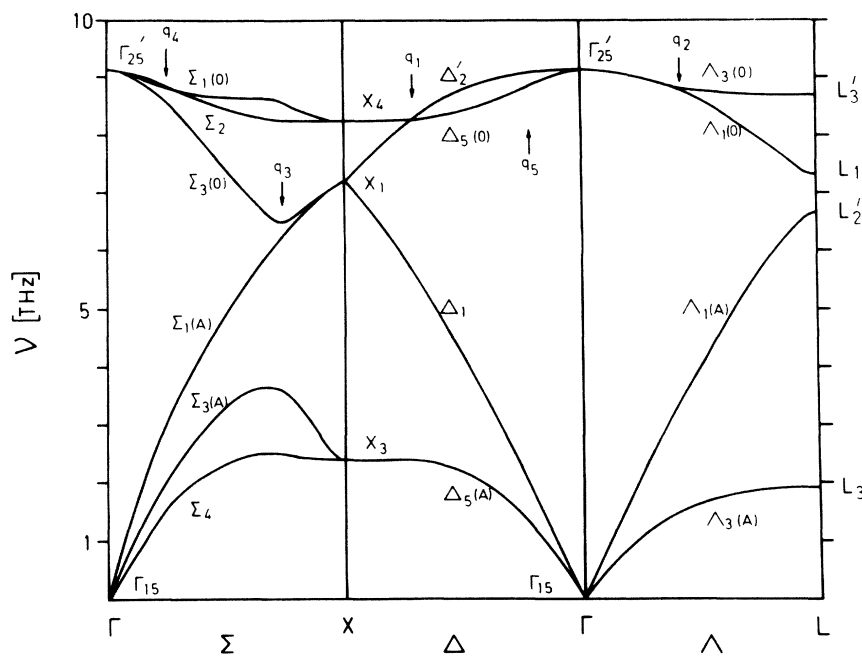


FIG. 3. Phonon dispersion relations in germanium at 80 K. The symbols  $q_i$  are explained in Sec. IV.

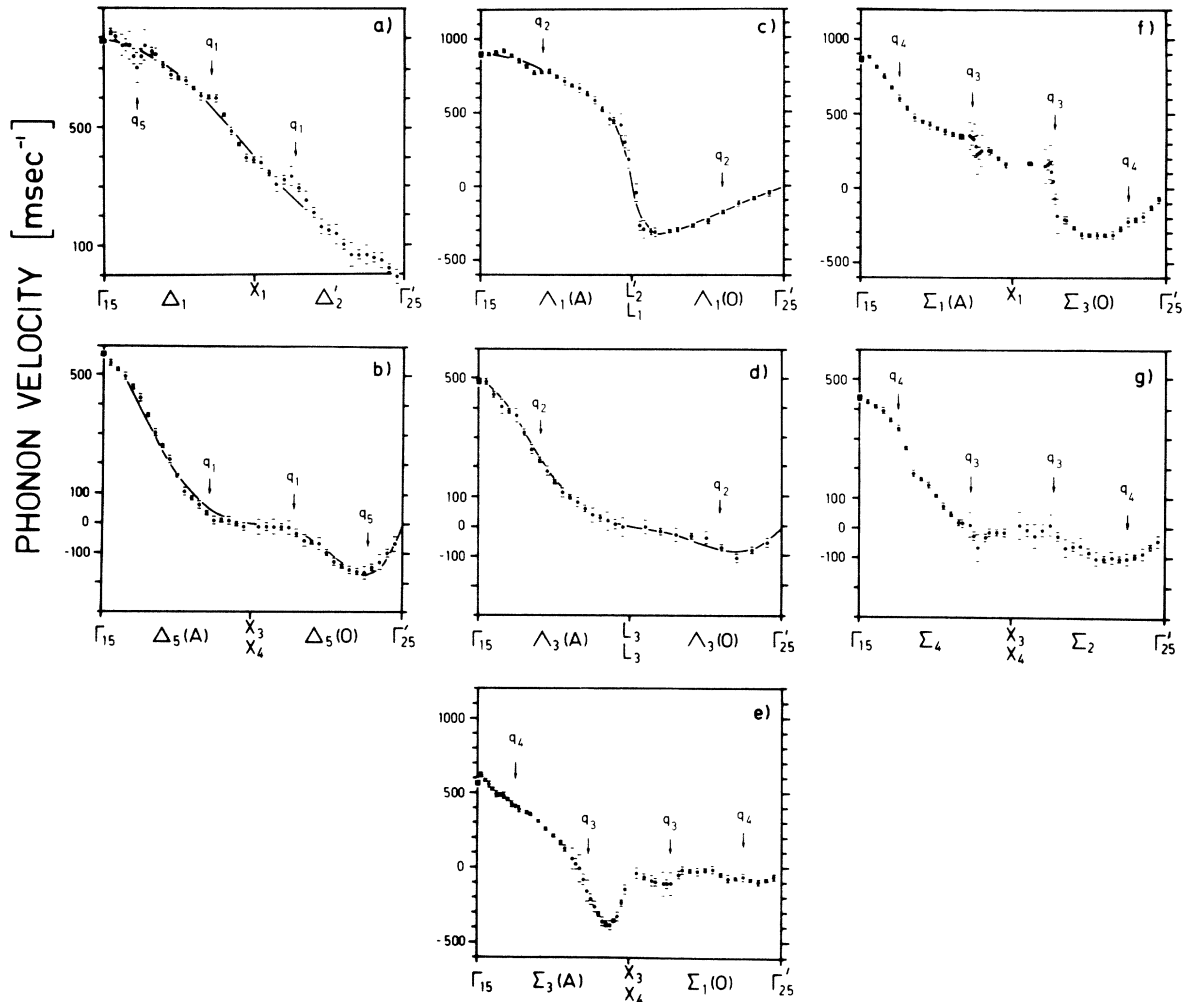


FIG. 4. Velocities of the phonon modes of the high-symmetry directions in germanium at 80 K as obtained by calculating the linear frequency gradients between both nearest and next-nearest points. (This means that the phonon velocity at  $\Gamma$  equals the velocity of sound divided by  $2\pi$ .) All published data (Ref. 3) have been utilized. The error bars mark the root mean squares of the experimental errors and the filled squares indicate the velocities of the acoustic modes in the long-wavelength limit as calculated from the elastic constants (Ref. 17). The solid curves and the symbols  $q_i$  are explained in Sec. IV.

should influence each other significantly. An observation of the removal of an accidental degeneracy may lie beyond the possibilities of present day neutron physics. However, according to Kagan and Zhernov even matrix elements belonging to wave vectors close to the one under consideration are affected by the anharmonicity so that anomalies or "kinks" are to be expected in the dispersion relations. Such effects are likely to be more easily observed than a removal of degeneracy. Cowley<sup>33</sup> has questioned the validity of the conjecture of Kagan and Zhernov. From a group-theoretical point of view it is difficult to understand why a perturbation with the same symmetry as the crystal should cause a coupling between phonons belonging to different irreducible representations. In fact, Kagan

and Zhernov tacitly assumed the existence of non-diagonal elements with this property. The symmetry properties of the phonon propagator for an arbitrary crystal have actually been studied by Maradudin and Ipatova.<sup>34</sup> Their work shows that nonvanishing off-diagonal elements only cause a coupling between solutions of specific modes. These are modes whose polarization vectors transform according to the same irreducible representation.

In the case of germanium at 80 K an inspection of Figs. 3 and 4 reveals the following:

(i) The wave vector of the accidental degeneracy between the branches  $\Delta'_2$  and  $\Delta_5(0)$  is marked by the symbol  $q_1$  in Figs. 3, 4(a), and 4(b). Pronounced kinks are observed at  $q_1$  in the gradients of the

well-separated branches  $\Delta'_2$  and  $\Delta_1$ . Within the limits of error, no kinks are clearly visible in the velocity curves for  $\Delta_5(A)$  and  $\Delta_5(0)$ , but they have a change in slope around  $q_1$ .

(ii)  $q_2$  marks the wave vector below which the two branches  $\Lambda_1(0)$  and  $\Lambda_3(0)$  could not be resolved. When a region of close contact is so extended, it is difficult to separate surmised anomalies from the general behavior of the curves [see Figs. 4(c) and 4(d)]. However, the velocity curve of the well-separated branch  $\Lambda_1(A)$  obviously possesses irregularities in the region considered. It is to be noted that the irreducible representation  $\Lambda_1$  corresponds to the same phonon polarization at  $\Delta_1$  and  $\Delta'_2$ , namely, the linearly polarized longitudinal mode. The representations  $\Lambda_3$  and  $\Delta_5$  are associated with the linearly polarized transverse mode.

(iii) Another region of close contact between two branches is afforded by  $\Sigma_1(A)$  and  $\Sigma_3(0)$ . The symbol  $q_3$  indicates the wave vector of minimum frequency for the branch  $\Sigma_3(0)$ . When passing through  $q_3$  the slope of the velocity curve changes for both  $\Sigma_1(A)$  and  $\Sigma_3(0)$ . The same effect is observed for all  $\Sigma$  branches except, maybe,  $\Sigma_3(A)$ . The larger scattering of points around  $q_3$  in Fig. 4 than elsewhere originates from the fact that phonon frequencies were determined for a more dense selection of wave vectors in this region.

(iv) The last region of interest in Fig. 3 is that marked by  $q_4$  at the point of accidental degeneracy between the elliptically polarized branch  $\Sigma_1(0)$  and the linearly transverse  $\Sigma_2$ . (All other branches are elliptically polarized, except that of  $\Sigma_4$ , which is linearly transverse.) Figures 4(e)–4(g) exhibit

nothing irregular at  $q_4$  with the possible exception of the branch  $\Sigma_4$ .

(v) Figure 4(a) shows an unexpected dip, marked  $q_5$ . Its origin may, perhaps, be connected with the fact that  $q_5$  coincides with the minimum of the velocity curve of  $\Delta_5(0)$  [see Fig. 4(b)]. As seen from Fig. 3, however, nothing noteworthy is present in any of the branches at  $q_5$ .

A nine-parameter version of the deformation dipole model,<sup>35</sup> which is equivalent to the shell model,<sup>36</sup> affords an excellent fit to the  $\Delta$  and the  $\Lambda$  branches of germanium at 80 K. This fit is even somewhat better than that of the valence-force-field model.<sup>31</sup> If the  $\Sigma$  direction is included, however, the good fit is lost. The velocity curves of the  $\Delta$  and the  $\Lambda$  branches as obtained from this fit are represented by solid lines in Figs. 4(a)–4(d). The kinks observed in the experimental results are obviously not compatible with this model.

In conclusion, the present analysis does not prove that the irregularities observed in the phonon gradients are of anharmonic origin. It indicates, however, that an accidental degeneracy or a close approach between branches may well influence the dispersion. The observed irregularities may also be explained on the basis of a more sophisticated harmonic model or in terms of a perturbation which does not share the crystal symmetry.

#### ACKNOWLEDGMENT

We are indebted to Dr. L. Bohlin for illuminating discussions on the problems dealt with in Sec. IV.

<sup>1</sup>R. T. Payne, Phys. Rev. Lett. **13**, 53 (1964).

<sup>2</sup>N. V. Zavaritskii, Zh. Eksp. Teor. Fiz. Pis'ma Red. **12**, 26 (1970) [Sov. Phys.-JETP Lett. **12**, 18 (1970)].

<sup>3</sup>G. Nilsson and G. Nelin, Phys. Rev. B **3**, 364 (1971).

<sup>4</sup>G. Nelin and G. Nilsson, Phys. Rev. B **5**, 3151 (1972).

<sup>5</sup>B. N. Brockhouse and B. A. Dasannacharya, Solid State Commun. **1**, 205 (1963).

<sup>6</sup>G. Dolling and R. A. Cowley, Proc. Phys. Soc. Lond. **88**, 463 (1966).

<sup>7</sup>R. A. Cowley, J. Phys. (Paris) **26**, 659 (1965).

<sup>8</sup>H. Jex, Phys. Status Solidi, B **45**, 343 (1971).

<sup>9</sup>H. Jex, Physics Lett. A **41**, 79 (1972).

<sup>10</sup>R. Stedman, L. Almqvist, G. Raunio, and G. Nilsson, Rev. Sci. Instrum. **40**, 249 (1969).

<sup>11</sup>F. Cerdeira and M. Cardona, Phys. Rev. B **5**, 1440 (1972).

<sup>12</sup>R. K. Ray, R. L. Aggarwal, and B. Lax, in Proceedings of the Second International Conference on Light Scattering in Solids, Paris, 1971, p. 288 (unpublished).

<sup>13</sup>J. H. Parker, Jr., D. W. Feldman, and M. Ashkin, Phys. Rev. **155**, 712 (1967).

<sup>14</sup>K. B. Tolpygo, Fiz. Tverd. Tela **3**, 943 (1961) [Sov. Phys.-Solid State **3**, 685 (1961)].

<sup>15</sup>R. H. Carr, R. D. McCammon, and G. K. White, Philos. Mag. **12**, 157 (1965).

<sup>16</sup>D. F. Gibbons, Phys. Rev. **112**, 136 (1958).

<sup>17</sup>H. J. McSkimin, J. Appl. Phys. **24**, 988 (1953).

<sup>18</sup>T. H. K. Barron, *Lattice Dynamics: Proceedings of an International Conference in Copenhagen* (Pergamon, New York, 1965), p. 247.

<sup>19</sup>J. L. Feldman, G. K. Horton, and J. B. Lurie, J. Phys. Chem. Solids **26**, 1507 (1965).

<sup>20</sup>G. K. Horton, Am. J. Phys. **36**, 93 (1968).

<sup>21</sup>P. Flubacher, A. J. Leadbetter, and J. A. Morrison, Philos. Mag. **4**, 273 (1959).

<sup>22</sup>G. Leibfried and W. Ludwig, Solid State Phys. **12**, 275 (1961).

<sup>23</sup>M. L. Cohen and T. K. Bergstresser, Phys. Rev. **141**, 789 (1966).

<sup>24</sup>K. Huang, *Statistical Mechanics* (Wiley, New York, 1963).

<sup>25</sup>H. S. Chen and D. Turnbull, J. Appl. Phys. **40**, 4214 (1969).

<sup>26</sup>U. Piesbergen, Z. Naturforsch. A **18**, 141 (1963).

<sup>27</sup>E. S. Greiner, J. Metals **4**, 1044 (1952).

<sup>28</sup>R. C. Smith, J. Appl. Phys. **37**, 4860 (1966).

<sup>29</sup>D. Gerlich, B. Abeles, and R. E. Miller, J. Appl. Phys. **36**, 76 (1965).

<sup>30</sup>A. W. Solbrig, Jr., J. Phys. Chem. Solids **32**, 1761 (1971).



<sup>31</sup>G. Nilsson and G. Nelin, Phys. Rev. B 6, 3777 (1972).

<sup>32</sup>Yu. Kagan and A. P. Zhernov, Zh. Eksp. Teor. Fiz. 48, 971 (1965) [Sov. Phys. -JETP 21, 646 (1965)].

<sup>33</sup>*Neutron Inelastic Scattering. Proceedings of a Symposium, Copenhagen* (IAEA, Vienna, 1968), Vol. I, p. 378.

<sup>34</sup>A. A. Maradudin and I. P. Ipatova, J. Math. Phys. 9,

525 (1968).

<sup>35</sup>Z. A. Demidenko, T. I. Kucher, and K. B. Tolpygo, Fiz. Tverd. Tela 3, 2482 (1961) [Sov. Phys. -Solid State 3, 1803 (1962)].

<sup>36</sup>W. Cochran, Proc. R. Soc. A 253, 260 (1959).